Supporting Information for

Structure, Solvent, and Relativistic Effects on the NMR Chemical Shifts in Square-Planar Transition-Metal Complexes: Assessment of DFT Approaches

Jan Vícha,[a,b,†] Jan Novotný,[a,†] Michal Straka,[a,c] Michal Repisky,[d] Kenneth Ruud,[d] Stanislav Komorovsky,[d,*] Radek Marek[a,e,*]

[a] *CEITEC – Central European Institute of Technology, Masaryk University, Kamenice 5/A4, CZ-62500 Brno, Czech Republic*

[b] *Centre of Polymer Systems, University Institute, Tomas Bata University in Zlin, Trida T. Bati, 5678, CZ-76001, Zlin, Czech Republic*

[c] *Institute of Organic Chemistry and Biochemistry, Academy of Sciences of the Czech Republic, Flemingovo nám. 2, CZ-16610 Prague, Czech Republic*

[d] *Centre for Theoretical and Computational Chemistry, Department of Chemistry, UiT – The Arctic University of Norway, N-9037 Tromsø, Norway*

[e] *Department of Chemistry, Faculty of Science, Masaryk University, Kamenice 5, CZ-62500 Brno, Czech Republic*

[†] These two authors contributed equally.

Corresponding Authors

E-mails: S. Komorovský: stanislav.komorovsky@uit.no, R. Marek: radek.marek@ceitec.muni.cz

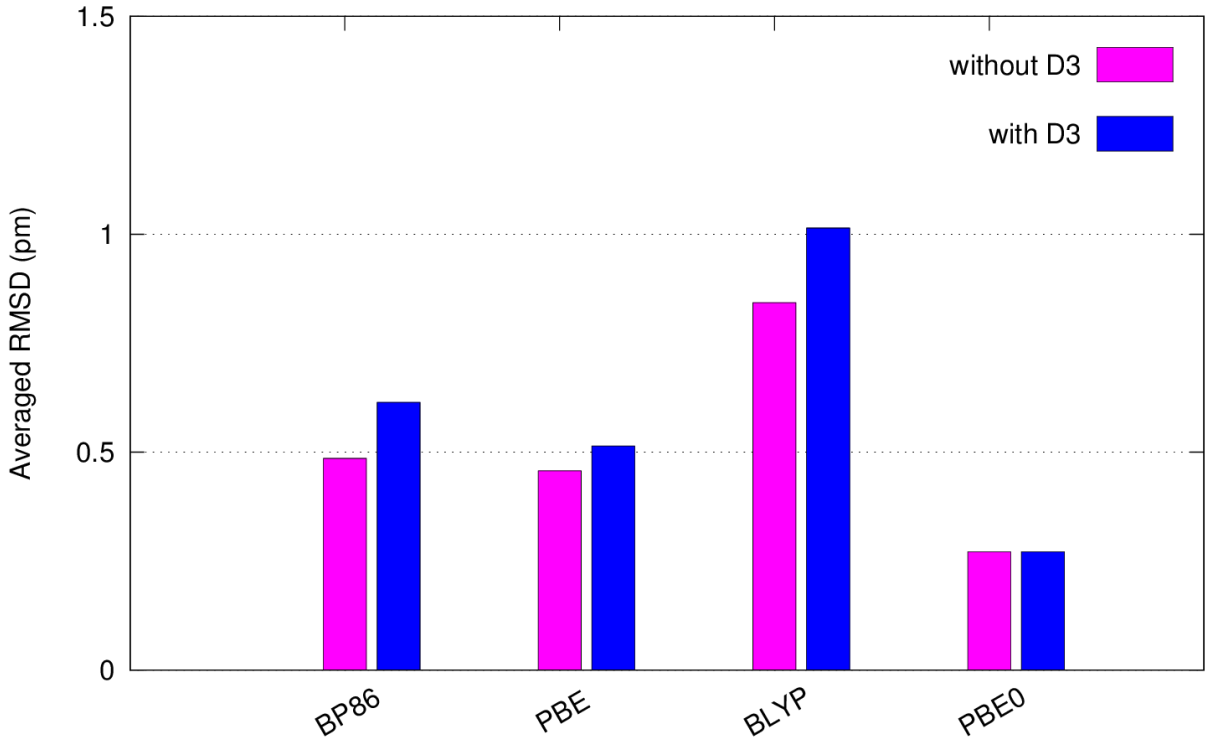

Figure S1. The total RMSDs (in pm) for all non-hydrogen bonds in Pt1 and Au1 relative to the experimental X-ray data, calculated using selected density functionals without (magenta) or with (blue) empirical D3 correction.

Performance of DFT functionals in geometry optimization - role of individual atomic types

Analysis of the data suggests that the performance of individual functionals is not much dependent on the type of metal center (see Figure S2), notable being only the results obtained for "distorted" Rh molecule, where GGA functionals BP86 and PBE perform better than PBE0.

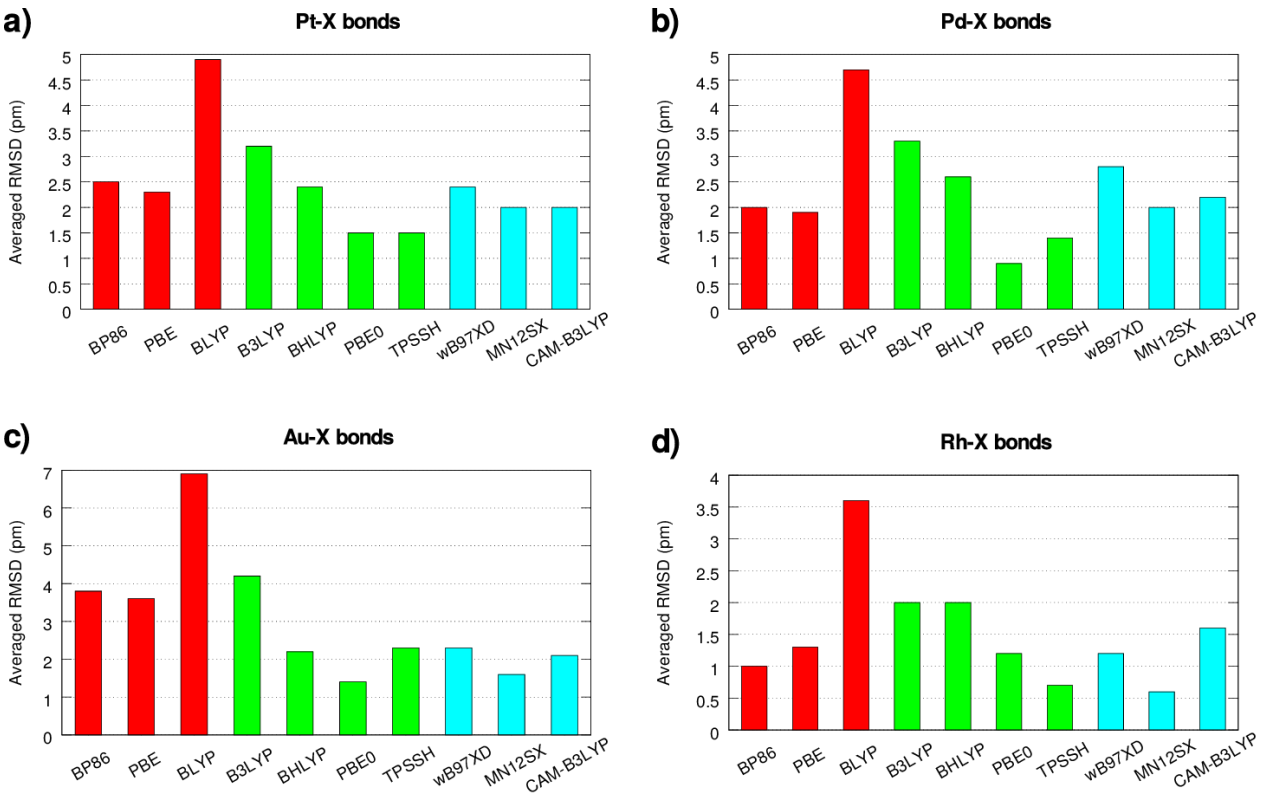

Figure S2. The RMSDs (pm) for the interatomic distances according to central metal a) platinum, b) gold c) palladium and d) rhodium relative to the experimental X-ray geometry calculated using various density functionals.

More interesting dependences are found when analyzing the data with respect to individual types of light ligand atoms (see Figure S3).

The M–N bonds are described equally well by all three best-performing functionals, while for M–C bonds TPSSh and MN12SX are performing slightly better than PBE0. On the contrary, M–P, M–S, and M–Cl bonds are reproduced considerably better by PBE0. Therefore, for molecules with C and N atoms bonded directly to transition-metal center, TPSSh (and MN12SX) would produce slightly better results than PBE0, whereas PBE0 is clearly outperforming all tested

functionals when bonding between central metal and heavier ligand atoms, such as Cl, S, and P is evaluated. Considering the importance of *trans* effect on the relativistic NMR parameters,[1] and because most of the atoms in *trans* position to spectator NMR atoms (usually ^{13}C or ^{15}N) in our testing set of complexes are heavier ones (mostly chlorines), the PBE0 functional was selected for the production geometry optimizations.

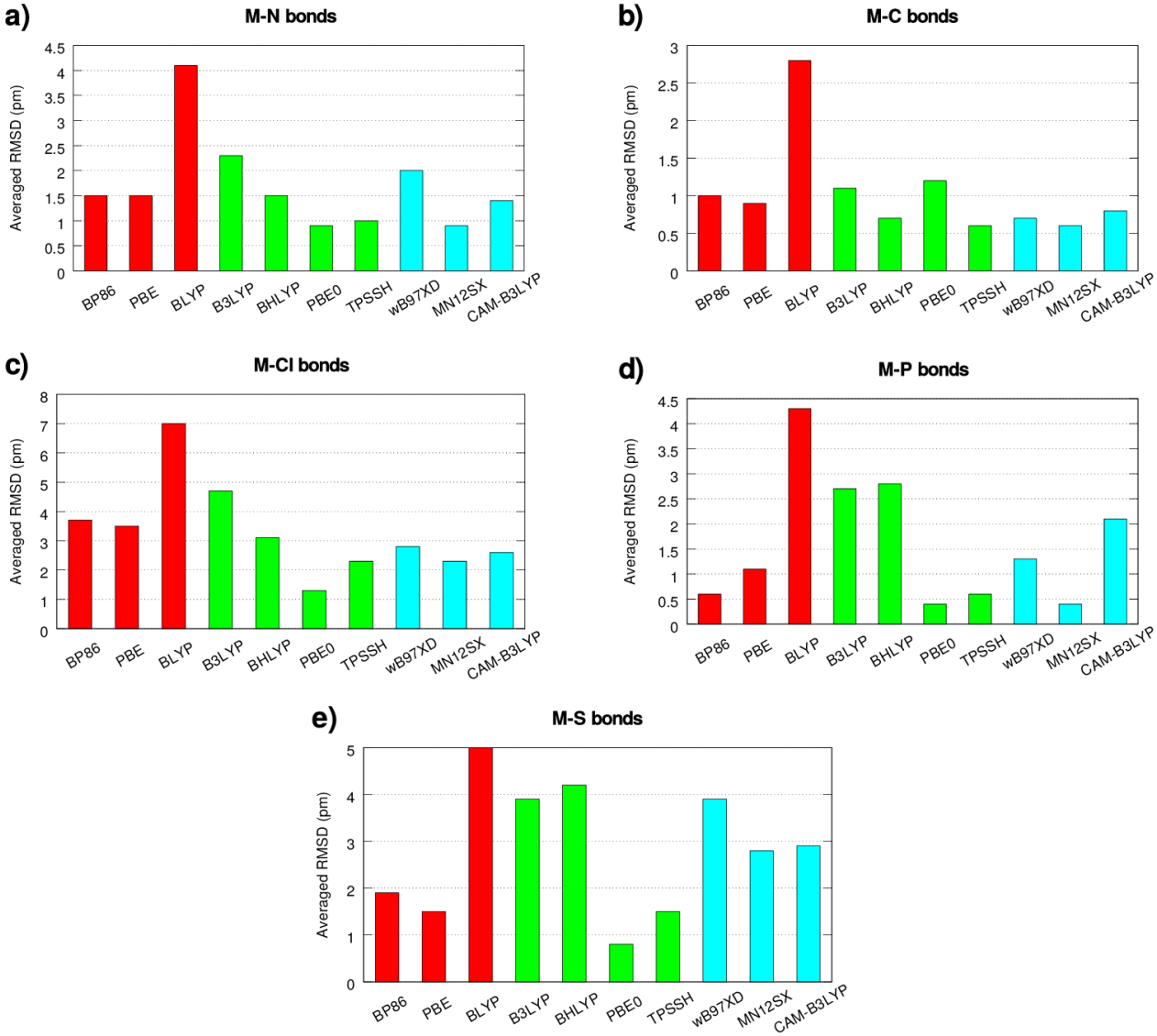

Figure S3. The RMSDs (pm) for the interatomic distances between central metal and a) nitrogen, b) carbon c) chlorine d) phosphorus, and e) sulfur relative to the experimental X-ray geometry calculated using various density functionals.

Role of cluster approach

To demonstrate the effect of crystal forces on the molecular geometry, the molecules were optimized *in vacuo* and resulting geometry was compared directly with that determined by X-ray diffraction (c.f. Table 1 in the main text). RMSD values are somewhat larger as compared to those for cluster optimizations, especially for M–L bonds, which is best documented by the results for the PBE0 functional, best performing in the cluster calculations. When the direct comparison between *in vacuo* geometries and X-ray structures is used, PBE0 results are on par with those for BP86 or PBE GGA functionals, seemingly disputing the need for the hybrid GGA functionals. However, the PBE0 was shown to produce much better results for instance in the case of M–Cl bonds than its GGA counterparts (which actually deviate more in the cluster), as demonstrated using cluster approach in Figure S4.

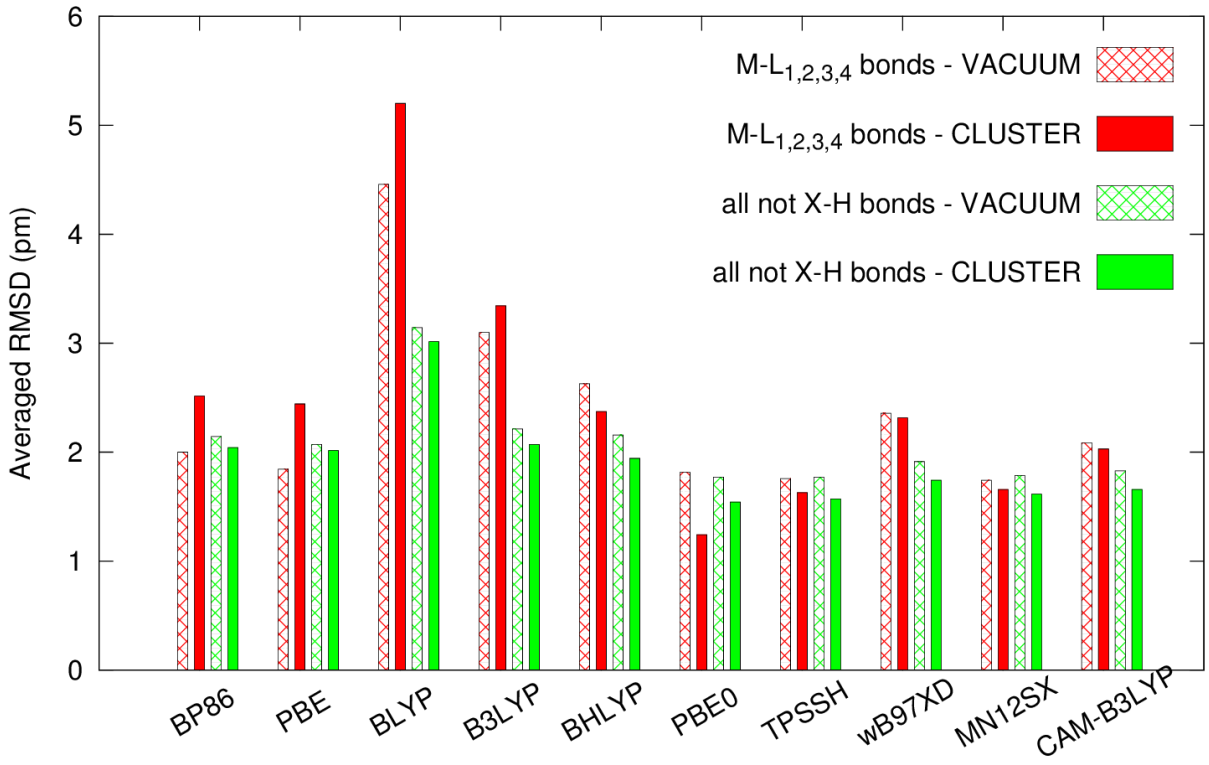

Figure S4. The total RMSDs (in pm) for interatomic distances relative to the experimental X-ray data, calculated using various density functionals. The M–L bonds (28) in red, all non-hydrogen bonds (161) in green calculated *in vacuo* (light colors) or in cluster (full colors).

Role of CGO correction in 4c mDKS approach

The poor basis-set convergence of CGO approach will result in ~ 10–20 ppm gauge-induced differences in calculated values (with gauge origin set to heavy element). To minimize the influence of the gauge dependence, empirical "CGO correction" obtained at the PBE level as difference between GIAO and CGO calculated shielding values ($\sigma_{PBE(CGO)}$ - $\sigma_{PBE(GIAO)}$) was implemented. This correction significantly improved otherwise severely underestimated results (see Figure S5) to the precision comparable with 2c GIAO calculations. The presented 4c PBE0 and PBE-40 results are used as a proof-of-concept, to demonstrate the capability of currently ongoing implementation of GIAO for the hybrid functionals. To confirm universal applicability of "CGO correction" calculations, however, further research on the extended testing set would be required.

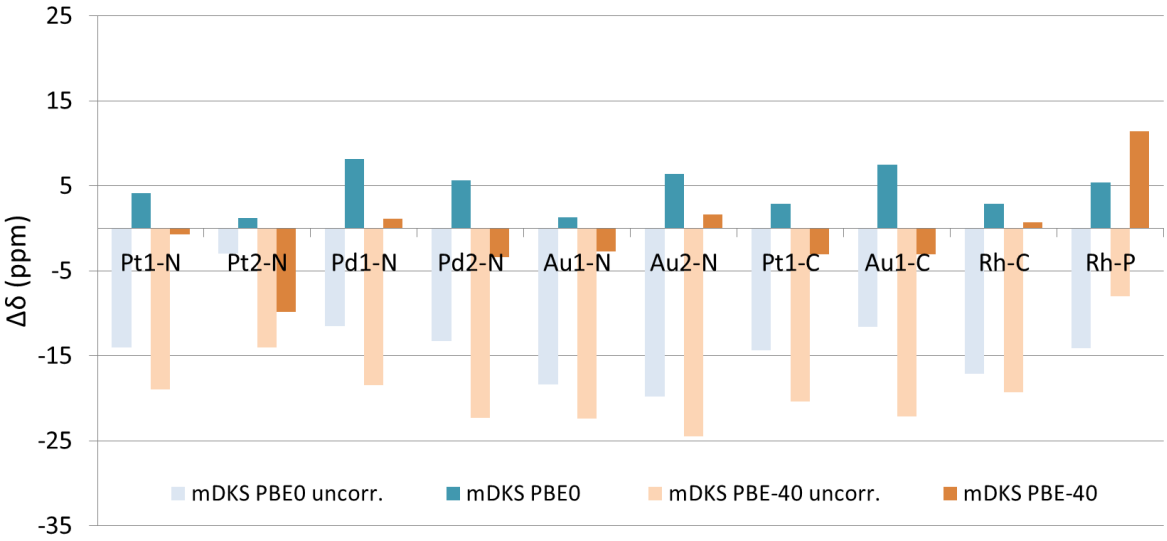

Figure S5. NMR chemical shifts calculated using mDKS PBE0 and mDKS PBE-40 approaches without (light colors) or with (dark colors) "CGO corrections".

Table S1. The NMR chemical shift differences (ppm) between calculated and experimental values obtained at various levels of theory, *in vacuo*.

Complex	2c-PBE	2c-PBE0	2c-PBE40	4c-PBE	4c-PBE0	4c-PBE40
Pt1-N	21.6	12.0	7.2	17.8	13.4	8.8
Pt2-N	28.3	11.0	1.1	23.2	9.1	-0.1
Pd1-N	21.2	24.1	23.6	19.3	26.3	25.0
Pd2-N	26.9	26.6	24.2	23.3	26.0	22.3
Au1-N	20.7	17.7	16.1	20.2	20.5	18.3
Au2-N	27.7	25.3	24.1	29.1	27.8	25.2
Pt1-C	21.4	8.7	1.5	16.0	8.1	1.9
Au1-C	20.7	11.8	5.8	18.3	11.7	1.5
Rh-C	5.6	2.9	0.1	6.2	3.9	1.4
Rh-P	-6.8	2.4	8.1	-4.8	5.3	10.5
RMSD	*21.4*	*16.5*	*14.6*	*19.2*	*17.5*	*15.1*

Table S2. The NMR chemical shift differences (ppm) between calculated and experimental values obtained at various levels of theory, COSMO model of solvent.

Complex	2c-PBE	2c-PBE0	2c-PBE40	4c-PBE	4c-PBE0	4c-PBE40
Pt1	13.6	2.8	-2.4	9.8	4.1	-0.7
Pt2	24.0	3.1	-8.6	18.9	1.2	-9.8
Pd1	13.6	5.9	-0.2	11.8	8.2	1.2
Pd2	17.9	6.3	-1.4	14.4	5.7	-3.4
Au1	5.4	-1.5	-4.8	5.0	1.3	-2.7
Au2	10.2	3.9	0.5	11.6	6.4	1.7
Pt1-C	15.4	3.5	-3.5	10.0	2.9	-3.1
Au1-C	16.3	7.6	1.2	13.9	7.5	-3.1
Rh-C	3.5	1.8	-0.6	4.1	2.8	0.7
Rh-P	-4.7	2.5	9.1	-6.7	5.4	11.4
RMSD	*13.9*	*4.4*	*4.5*	*11.5*	*5.1*	*5.2*

Table S3. Exchange-correlation DFT kernel values ($\Delta\delta^{XC}_{kernel}$) obtained using PBE functional with 0, 25, or 40% of exact-exchange admixture.

Atom	$\Delta\delta^{XC}_{kernel}$ at 4c level		
	PBE	PBE-25	PBE-40
Pt1-N	-2.3	-3.0	-2.9
Pt2-N	-2.2	-3.2	-2.9
Pd1-N	-1.3	-0.8	-0.7
Pd2-N	-3.1	-1.6	-1.6
Au1-N	0.3	0.9	0.8
Au2-N	-0.9	2.8	2.7
Pt1-C	-5.2	-5.6	-5.3
Au1-C	-4.0	-3.6	-3.9
Rh-C	-1.2	-1.3	-1.3
Rh-P	-1.1	-2.4	-1.9

References:

(1) Vícha, J.; Straka, M.; Munzarová, M. L.; Marek, R. *J. Chem. Theory Comput.* **2014**, *10* (4), 1489–1499.